HHS Public Access

Author manuscript

J Immunol. Author manuscript; available in PMC 2020 January 15.

Published in final edited form as:

J Immunol. 2019 January 15; 202(2): 484–493. doi:10.4049/jimmunol.1701433.

Influenza A Virus Infection Induces Muscle Wasting via IL-6 Regulation of the E3 Ubiquitin Ligase Atrogin-1

Kathryn A. Radigan[*,†], **Trevor T. Nicholson**[*,†], **Lynn C. Welch**[*,†], **Monica Chi**[†], **Luciano Amarelle**[†], **Martín Angulo**[†,‡], **Masahiko Shigemura**[†], **Atsuko Shigemura**[†], **Constance E. Runyan**[†], **Luisa Morales-Nebreda**[†], **Harris Perlman**[†], **Ermelinda Ceco**[†], **Emilia Lecuona**[†], **Laura A. Dada**[†], **Alexander V. Misharin**[†], **Gokhan M. Mutlu**[§], **Jacob I. Sznajder**[†,¶], and **G.R. Scott Budinger**[†,¶]

[†]Department of Medicine, Feinberg School of Medicine, Division of Pulmonary and Critical Care Medicine, Northwestern University, Chicago, IL, USA

[‡]Departamento de Fisiopatología, Facultad de Medicina, Universidad de la República, Montevideo, Uruguay

[§]University of Chicago, Section of Pulmonary and Critical Care Medicine, Chicago, IL, USA

Abstract

Muscle dysfunction is common in patients with ARDS and is associated with morbidity that can persist for years after discharge. In a mouse model of severe influenza A pneumonia, we found the pro-inflammatory cytokine IL-6 was necessary for the development of muscle dysfunction. Treatment with an FDA approved antibody antagonist to the IL-6 receptor (tocilizumab) attenuated the severity of influenza A-induced muscle dysfunction. In cultured myotubes, IL-6 promoted muscle degradation via JAK/STAT, FOXO3a and atrogin-1 upregulation. Consistent with these findings, *atrogin-1* $^{+/-}$ and *atrogin-1* $^{-/-}$ mice had attenuated muscle dysfunction following influenza infection. Our data suggest that inflammatory endocrine signals originating from the injured lung activate signaling pathways in the muscle that induce dysfunction. Inhibiting these pathways may limit morbidity in patients with influenza A pneumonia and ARDS.

Introduction

Influenza A pneumonia is the most common cause of morbidity from an infectious agent responsible for at least 20,000 to 50,000 deaths in the United States yearly (1, 2). The lung epithelium is the primary target of the influenza A virus (IAV) infection, and the resulting diffuse damage to the epithelium can impair gas exchange resulting in severe pneumonia and development of the Acute Respiratory Distress Syndrome (ARDS). About 30–40% of patients with ARDS die, and most survivors often suffer multiple morbidities related to their prolonged critical illness (3, 4). Muscle weakness is evident in up to 50% of ARDS survivors, where it is associated with prolonged lengths of stay in the intensive care unit and

[¶]Address correspondence and reprint requests to: Jacob I. Sznajder or G.R. Scott Budinger, 240 E. Huron St. McGaw M300, Chicago, IL 60611 USA, Phone: 312-908-7737, Fax: 312-503-0411, j-sznajder@northwestern.edu or s-buding@northwestern.edu.
[*]Denotes first co-authors

the development of the multiple organ dysfunction syndrome (5–7). In patients who survive ARDS, muscle weakness results in substantial morbidity and long-term reductions in quality of life (8–11).

As survival from ARDS continues to improve (12, 13), it is increasingly important to prevent muscle dysfunction and other long-term sequelae of the syndrome (14). Our understanding of the pathophysiology of muscle weakness associated with critical illness is incomplete. Some investigators have argued that skeletal muscle dysfunction in ARDS is largely attributable to the prolonged immobility associated with critical illness (14, 15). Others have shown that the ubiquitin proteasome system is activated in skeletal muscle within hours or days of the onset of critical illness, suggesting a role for active signaling processes that promote muscle dysfunction (7, 16).

Maintenance of muscle mass requires an equilibrium between the synthesis and breakdown of myofiber proteins. Muscle atrophy occurs when there is a net loss of muscle mass causing shrinkage of the myofibers. There are several different types of skeletal muscle atrophy including, sarcopenia, disuse atrophy and cachexia (9, 10, 17). The FoxO (forkhead box O) class of transcription factors have been implicated in the control of muscle degradation (18, 19). Specifically, FoxO1 and FoxO3 upregulate the muscle-specific ubiquitin ligases: MAFbx/atrogin-1 (muscle atrophy F-box protein) and MuRF1 (muscle RING finger-1), which target muscle proteins for degradation by the ubiquitin proteasome system (20, 21). The pro-inflammatory cytokine IL-6 has been reported to regulate atrogin-1 and thus promote muscle atrophy (22–24). Cellular signaling induced by IL-6 has been shown to activate the Janus kinases (JAK)/signal transducer and activator of transcription 3 (STAT3) (25). Phosphorylation of STAT3 leads to the translocation of (FoxO)3 to the nucleus leading to upregulation of atrogin-1 (19, 26).

In animal models and healthy volunteers infected with influenza A virus, IL-6 and TNF-α are rapidly detected in bronchoalveolar lavage fluid and nasal washings (27, 28). IL-6 is also increased in the serum of patients with lung injury (29, 30), and in mouse models of influenza infection (28). Increased levels of IL-6 and other inflammatory cytokines are associated with prolonged mechanical ventilation (29, 30) and increased mortality (29–31). In this study, we sought to determine whether IL-6-mediated activation of STAT3/atrogin-1 was necessary for the development of muscle dysfunction in a murine model of influenza A infection.

Materials and Methods

Reagents

All cell culture reagents were from Corning Life Sciences (Tewksbury, MA). All other chemicals were purchased from Sigma-Aldrich (St. Louis, MO).

Mice

Adult male (12–16 weeks) C57Bl/6 wild-type were obtained from The Jackson Laboratories (Bar Harbor, ME). Age-matched male *atrogin-1*$^{-/-}$ and *atrogin-1*$^{+/-}$ mice as well as wild-type littermates (*atrogin-1* $^{+/+}$) on a 129S/C57Bl/6 background have been described

previously and were obtained from Regeneron Pharmaceuticals and Stewart Lecker at Beth Israel Deaconess Medical Center and Harvard Medical School (20). Mice were provided with food and water *ad libitum*, maintained on a 14-h light/10-h dark cycle, and handled according to National Institutes of Health and Northwestern University Institutional Animal Care and Use Committee guidelines. Northwestern University Institutional Animal Care and Use Committee approved all animal experimental protocols.

Influenza A Virus and Infection

Influenza A virus (A/WSN/33 [H1N1]), a murine adapted virus, was provided by Robert Lamb, Ph.D., Sc.D., Northwestern University, Evanston, IL. Mice were anesthetized with isoflurane, their lungs were intubated with a 20-gauge angiocath (32, 33) and two 25 μl sterile aliquots of Phosphate Buffered Saline ((PBS) Control) or influenza A virus (A/WSN/33 [H1N1]) (1500 or 150 pfu/mouse) were instilled through the catheter as we have previously described (28). We continuously observed mice infected with influenza A virus for signs of distress (slowed respiration, failure to respond to cage tapping, failure of grooming, huddling and fur ruffling). Mice that developed these symptoms were sacrificed and the death was recorded as an influenza A-induced mortality. Weight was measured at infection time and prior to harvest 7 days post-infection (dpi) and recorded as percentage of weight loss from baseline.

Administration of tocilizumab

Tocilizumab is a humanized monoclonal antibody against the interleukin-6 (IL-6) receptor; for our studies, we used a murine adapted form of tociluzimab (Genentech, South San Francisco, CA). Briefly, adult male C57Bl/6 mice were anesthetized with isoflurane and were administered tocilizumab 8mg/kg in a total volume of 150 μl of PBS or PBS alone by a retro-orbital injection. After 24 hours, the mice were infected with IAV or PBS as described above.

Measurement of muscle dysfunction

Immediately prior to muscle harvest, forelimb skeletal muscle strength was assessed using a digital grip strength meter (Columbus Instruments, Columbus, OH) as described (34, 35). Grip strength was measured in each animal six successive times, and the average of the highest four values for each mouse was used. The same operator performed all tests. The mice were then terminally anesthetized with Euthasol (pentobarbital sodium/phenytoin sodium). The soleus and extensor digitorum longus (EDL) muscles were excised and tendon was trimmed under a microscope to assure optimal accuracy for weight measurement. The muscles were then blotted dry and weighed. Muscles were either frozen in liquid nitrogen-cooled isopentane for cryosectioning or snap-frozen in liquid nitrogen for protein extraction.

Immunohistochemistry and Fiber Size Assessment

Soleus and EDL serial transverse cryosections (8 μm) were obtained from the Northwestern University Mouse Histology and Phenotyping Laboratory and mounted on glass slides. Sections were fixed in 4% formaldehyde, permeabilized, and blocked. Immunostaining was performed with laminin primary antibody (Sigma; Catalog: L9393; 1:50) followed by Alexa

Fluor 568-conjugated secondary antibody (Life Technologies, Carlsbad, CA; Catalog: A-11011; 1:200). Images were acquired with a Zeiss LSM 510 confocal microscope using a 40x objective (Northwestern University Center for Advanced Microscopy) and analyzed using Fiji (National Institutes of Health) (36). Fiber size and cross-sectional area (CSA) were determined as previously described (34). All analysis was performed by one blinded-operator.

Cell Culture, siRNA Transfection, Drug Treatment, Myotube Analysis and Viral Plaque Assay

C2C12 mouse myoblasts (ATCC, Manassas, VA: CRL-1772) were cultured and differentiated as we have previously have described (34). For experimental procedures, myoblasts were grown to 90–95% confluence and then media was switched to 2% horse serum DMEM (differentiation media) and renewed daily for optimal myotube formation. For siRNA transfection experiments, 90–95% confluent C2C12 myoblasts were switched to differentiation media (Day 0). On Day 1 of differentiation, the media was replaced with antibiotic-free differentiation media and transfection protocol was performed 12 hours later. On day 2 of differentiation, cells were transfected with 60 ρmol of either mouse *STAT3, FKHRL1, FKHR,* or control siRNA (Scramb) pools (Santa Cruz Biotechnology, Dallas, TX) using Lipofectamine RNAiMax Transfection reagent (Thermo Fisher Scientific, Waltham, MA) according to the manufacturer's instructions. On day 4 of differentiation, cells were treated with 10 ng/ml of recombinant mouse IL-6 (BD Biosciences, San Jose, CA) for 16 hours. For the dose-response treatment of IL-6, cells were treated on day 4 of differentiation with various concentrations IL-6 (2.5, 5 and 10 ng/ml) for 16 hours. For experiments with tocilizumab, cells were treated with 10 μg/ml on Day 3 for 24 hours followed by treatment on Day 4 of differentiation with 10 ng/ml of recombinant mouse IL-6 for 16 hours. C2C12 myotubes were treated on day 4 with 2 MOI of influenza A virus (A/WSN/33 [H1N1]) for 16 hours. On day 5 of differentiation, cells were imaged and then cell lysates were obtained for Western blot analysis. Images were acquired using a Nikon Eclipse TE2000-U inverted scope with a 40X objective. Myotube diameters were quantified by one blinded-operator measuring ~375–679 tube diameters (5–10 measurements per fiber) from five random fields from a minimum of 3 independent experiments using MetaMorph Software (Molecular Devices, Sunnyvale, CA; Version 6.3) as previously described (34). Madin-Darby Canine Kidney (MDCK) cells (ATCC,CCL-34) cells were maintained as described previously and used to perform a viral plaque assay with homogenized soleus muscle or lungs from mice infected with influenza (37).

Western Blot Analysis

C2C12 myotubes were washed with ice-cold PBS and then lysed with 2X Cell Lysis Buffer (Cell Signaling Technology, Danvers, MA). Lysates were centrifuged at 20,000 x g and the supernatant was collected. Soleus and EDL muscles were lysed with ice-cold lysis buffer (Nonidet P-40 1%, glycerol 10%, NaCl 137 mM, Tris-HCl pH 7.5 20 mM) containing protease (1 Complete Mini, EDTA-free tablet, Roche) and phosphatase (sodium fluoride 30 mM, β-glycerophospate 250 mM, sodium orthovanadate 1mM) inhibitors (38). Tissue was then homogenized with a Tissue Tearor (BioSpec Products, Inc, Bartlesville, OK) for 1 minute. Samples were centrifuged at 15,000 rpm for 10 minutes at 4° C and the supernatant

was collected. Protein concentrations were determined with Protein Assay Dye (Bio-Rad, Hercules, CA) using the Bradford method (39). Equal amount of protein were loaded on a SDS-PAGE and Western blot analysis was performed as described previously (40). Incubation with primary antibodies was performed overnight at 4°C. Immunoblots were quantified by densitometry using Image J 1.46r (National Institutes of Health) or Image Studio Software (LI-COR Inc., Lincoln, NE) (41). The following antibodies were used: Rabbit Monoclonal to Fbx32 (Abcam, Cambridge, United Kingdom; catalog: ab168372; 1:1000), Rabbit polyclonal to MuRF1 (ECM Biosciences, Versailles, KY; catalog: MP3401; 1:1000), Rabbit monoclonal to GAPDH (D16H11) (Cell Signaling; catalog: 5174s; 1:1000), Rabbit monoclonal to STAT3 (79D7) (Cell Signaling; catalog: 4904s; 1:1000), Rabbit monoclonal to FoxO3a (75D8) (Cell Signaling; catalog: 2497s; 1:1000), Rabbit polyclonal to FoxO1 (L27) (Cell Signaling: catalog: 9454s; 1:1000). Primary antibodies were detected with horseradish peroxidase-conjugated secondary antibodies including Anti-Rabbit IgG, HRP-linked (Cell Signaling: catalog: 7074s; 1:2000 dilution) and Goat-Anti-Rabbit IgG-HRP conjugate (Bio-Rad: catalog: 170–6515; 1:16,000 dilution).

Bronchoalveolar lavage (BAL) fluid and blood collection for measurement of cell count, protein and IL-6.

Animals were euthanized with Euthasol (pentobarbital sodium/phenytoin sodium) prior to BAL and blood collection. A mid-line dissection through the abdominal cavity up to the thoracic cavity was performed followed by a small incision at the edge of the diaphragm, which resulted in a fatal pneumothorax. Then, a right ventricular puncture for the collection of blood was performed. Blood was collected in a microvette microtube with EDTA (Kent Scientific) and kept on ice and then spun at 2000 rpm. Serum was collected and used for IL-6 determination by ELISA (Thermo Fisher, KMC0062) (37). Bronchoalveolar lavage (BAL) fluid was obtained through a 20-gauge angiocath ligated into the trachea through a tracheostomy. A total of 1-ml of PBS instilled into the lungs was aspirated three times to collect BAL fluid for cell counts (Cellometer K2; Nexcelom Bioscience), protein quantification (Bradford assay) and IL-6 determination by ELISA.

Statistics

Results are shown as mean ± SEM. Data were analyzed and statistical differences were compared by a Student's *t*-test between two groups and by a one-way ANOVA with Dunnett or Tukey's post-hoc corrections for three or more groups using GraphPad Prism version 7.0 for Windows (GraphPad Software, La Jolla, CA). All *in vitro* experiments were repeated a minimum of three times. We considered specific data points outliers if they deviated by more than two times the standard deviation from the mean and they were excluded automatically from the statistical analysis. Results were considered significant when p value < 0.05.

Results

C57Bl/6 wild-type mice lose muscle weight and strength after influenza infection.

We infected C57Bl/6 wild-type mice with either a low dose (150 pfu/mouse) or high dose (1500 pfu/mouse) of influenza A virus (A/WSN/33 [H1N1]) (IAV) and assessed total body

weight, forelimb grip strength, soleus and EDL muscle wet weight, and fiber cross-sectional area (CSA). Compared to control (PBS-treated) mice, IAV-infected mice experienced significant weight loss after both low dose and high dose IAV infection (Figure 1A). Forelimb grip strength was significantly decreased in the IAV-infected mice (Figure 1B). In addition, mice-infected with either low or high dose influenza had significantly decreased soleus and EDL wet muscle weight (Figure 1C, 1D). Figure 1E and 1H show representative images of soleus and EDL laminin-stained cryosections that were used to determine the mean CSA. Mice infected with high dose IAV had significantly decreased mean soleus and EDL CSA (Figure 1F, 1I) with the histograms showing a left shift of frequency distribution indicating a predominance of thinner fibers in IAV-infected mice (Figure 1G, 1J).

To determine that the IAV infection was restricted to the lung, we measured by plaque assay the viral load in lungs and soleus muscle of mice infected with IAV for 7 days. As expected the viral load was almost undetectable in soleus muscle homogenates compared with lung homogenates of wild-type IAV-infected mice (soleus: 38.33 pfu/ml ±6.009 S.E.M.; lung: 1.25×10^7 pfu/ml $\pm 8.3660 \times 10^5$ S.E.M.). A Student's *t*-test between two groups was used to show statistical differences with a $p<0.0001$ (n=3–5 mice/group).

Influenza-induced muscle dysfunction is attenuated in mice with genetic loss of atrogin-1.

The ubiquitin-proteasome system regulates muscle degradation via the E3 ubiquitin ligases, MAFbx/atrogin-1 and MuRF1 (20, 21). We set out to determine if either or both of these muscle specific-E3 ubiqutin ligases were up-regulated in our murine model of IAV infection. C57Bl/6 wild-type mice were infected with IAV (1500 pfu/mouse) and 7 days dpi the mice were sacrificed and the soleus muscles were excised. We found that atrogin-1 protein expression was significantly increased while MuRF1 levels remained unchanged (Figure 2A, 2B). To further explore the role of atrogin-1 in mediating muscle protein loss with influenza, we used mice with heterozygous or homozygous deletion of the *MAFBx/atrogin-1* gene (designated as *atrogin-1* throughout the paper) (20). Compared with their wild-type (*atrogin-1*$^{+/+}$) littermates, levels of atrogin-1 were significantly lower in the soleus muscle of *atrogin-1*$^{+/-}$ and *atrogin-1*$^{-/-}$ mice (Figure 2C). Phenotypic differences in the animals were also evident. Basally, *atrogin-1*$^{+/-}$ had slightly reduced grip strength but was not statically different as compared to the PBS-treated *atrogin-1*$^{+/+}$. *Atrogin-1*$^{-/-}$ mice baseline grip strengths were markedly decreased, but there was no difference between control (PBS-treated) and IAV-treated mice, suggesting that lower levels of atrogin-1 are protective during influenza infection (Figure 2D). While *atrogin-1*$^{+/+}$ had significantly decreased wet muscle weight for soleus and EDL after IAV infection, wet muscle weight after influenza A infection was similar to uninfected mice in the *atrogin-1*$^{-/-}$ mice (Figure 2E-F). The haploinsufficient *atrogin-1*$^{+/-}$ mice showed levels of wet muscle weight loss intermediate between *atrogin-1*$^{+/+}$and *atrogin-1*$^{-/-}$(Figure 2E-F). The mean fiber CSA for the soleus and EDL muscles were decreased in the *atrogin-1*$^{+/+}$ IAV-infected mice as compared to control (PBS-treated) mice, but the IAV-induced decrease in CSA was attenuated *atrogin-1*$^{+/-}$ and *atrogin-1*$^{-/-}$ mice (Figure 2G-P). Each of the *atrogin-1* genotypes infected with IAV lost body weight as compared to the PBS-treated mice, but the *atrogin-1*$^{+/-}$ and *atrogin-1*$^{-/-}$ weight loss was slightly less severe (Figure 3A).

Additionally, IL-6 levels were measured in serum and bronchoalveolar lavage (BAL) fluid. Total protein and cell count were also determined in the BAL fluid. IL-6 levels were markedly increased in the IAV-infected *atrogin-1*$^{-/-}$ in both serum and BAL fluid as compared to IAV-infected *atrogin-1*$^{+/-}$ and *atrogin-1*$^{-/-}$ mice (3B and 3C). There was no difference amongst the different *atrogin-1* genotypes infected with IAV in total protein and cell count of the BAL fluid (3D and 3E).

The IL-6-receptor antibody tocilizumab attenuates influenza-induced muscle dysfunction.

To investigate the role of IL-6 in mediating influenza A-induced muscle atrophy *in vivo*, we treated C57Bl/6 mice with tocilizumab, which is a monoclonal antibody with specificity for the IL-6 receptor that prevents IL-6 from binding to both the soluble and membrane-bound IL-6 receptor through competitive blockade (42). C57Bl/6 mice were administered tocilizumab 8mg/kg or PBS (control) 24 hours by retro-orbital injection prior to infection with IAV (1500 pfu/mouse) or PBS and then 7 dpi weight loss and grip strength were assessed. There was no difference in total body IAV-induced weight loss between the PBS- and tocilizumab-treated mice (Figure 4A). The reduction of grip strength observed in IAV-infected mice treated with vehicle was attenuated in the IAV-infected and tocilizumab treated mice (Figure 4B). Consistent with these findings, soleus and EDL wet muscle weights were significantly reduced in influenza-infected compared with uninfected wild-type mice, while there was no significant decrease in either the soleus or EDL wet muscle weight in uninfected compared with tocilizumab treated mice (Figure 4C, 4D). The influenza A-induced induction of atrogin-1 protein was attenuated in the soleus muscle of tocilizumab-treated mice (Figure 4D). Similarly, the influenza A-induced reductions in soleus and EDL CSA were attenuated in mice that had been pre-treated with tocilizumab compared with vehicle as was the left-shift of muscle fiber size frequency distribution for both the soleus and EDL (Figure 4F-M).

IL-6 acts via STAT3, FoxO3a, and Atrogin-1 to induce skeletal muscle atrophy

To obtain insight into the mechanisms by which IL-6 induces muscle atrophy, we treated differentiated C2C12 myotubes with various doses of recombinant IL-6 (2.5, 5 and 10 ng/ml) or with 1 MOI of IAV or media alone, and blinded measurements of myotube diameters were performed 16 hours later. Treatment of C2C12 cells with IL-6 resulted in a dose-dependent reduction in myotube diameter, while treatment with IAV had no effect on fiber diameter (Figure 5A). To determine if STAT3 was involved in the IL-6-induced reduction in myotube diameter, we transfected well-differentiated C2C12 cells with scrambled siRNA or siRNA specific for *STAT3* followed by treatment with recombinant IL-6 and then measured myotube diameters. Silencing of STAT3 prevented the decrease in diameter seen with IL-6 treatment (Figure 5B). To determine whether STAT3 acts through FoxO1 or FoxO3a to reduce myotube diameter, we compared the effect of IL-6 on myotube diameter in control, FoxO1 and FoxO3a silenced cells. Silencing of FoxO3a attenuated the decline in myotube diameter induced by IL-6 (Figure 5C), but silencing of FoxO1 did not prevent the decrease in myotube diameter (Figure 5D). Consistent with our *in vivo* findings, pretreatment of myotubes with tocilizumab prevented the IL-6-induced decrease in myotube diameter as compared to the myotubes that received the mock treatment and IL-6 (Figure 5E). Moreover, treatment of myotubes with IL-6 increased the expression of atrogin-1 in

vehicle treated cells and this effect was attenuated in cells pretreated with tociluzumab (Figure 5F).

Discussion

Severe infection with the influenza A virus is an important cause of lung injury and ARDS (1, 2). A significant proportion of patients with ARDS develop skeletal muscle weakness that is associated with prolonged duration of mechanical ventilation and with increased short-term and long-term mortality (43, 44). In patients who survive ARDS, muscle dysfunction may persist for years after hospital discharge, impairing quality of life and affecting survival (1, 2, 9, 10, 17). Using a murine model of influenza A infection, we show that IL-6 released from the influenza A infected lung upregulates atrogin-1 to promote the active degradation of muscle proteins via the ubiquitin-proteasome pathway. Muscle mass and function could be preserved during influenza A infection through genetic deletion of atrogin-1 or through pharmacologic blockade of the IL-6 receptor. The fact that mice infected with IAV had negligible viral load detected in the soleus muscle homogenates and that differentiated C2C12 mouse myotubes have reduced muscle fiber size when treated with IL-6 and not when incubated with IAV, suggest an endocrine mechanism for the muscle loss observed in influenza A infected mice. The effects of IL-6 on fiber size were attenuated by knockdown of STAT3 or FoxO3a and by pharmacologic inhibition of the IL-6 receptor, but not with knockdown of FoxO1. These data suggest that muscle loss during influenza A infection is an active process initiated by endocrine signals from the injured lung.

Our data in mice are potentially relevant for humans. IL-6 and TNF-α are the first detectable cytokines after influenza infection (27, 37), and are increased in the serum of patients with lung injury (29–31). In humans with influenza A infection, IL-6 levels peak within 2 days of infection, and remain elevated for up to 7 days, with levels that correlate with symptom severity (27). In patients with ARDS, the activation of proteolytic pathways follows a similar time course, with increases in ubiquitination of muscle proteins detected within hours of onset of critical illness and remaining active for up to one week following discharge from the ICU (7, 45). Our *in vivo* measurements were performed at 1 week following infection of the influenza A virus (A/WSN/33 [H1N1]) administered intratracheally, at which point proteolytic pathways are active and muscle weakness is evident. In *atrogin-1* mice, we observed an increase in IL-6 in both serum and bronchoalveolar lavage fluid after IAV infected in all the genotypes, but even though it was profoundly increased in the *atrogin-1* $^{-/-}$ mice the lack of atrogin-1 in the muscle is enough to protect against muscle atrophy.

While our studies demonstrate a deleterious role for IL-6 during IAV-induced lung injury, IL-6 can also be produced by muscle fibers during exercise where it acts as a myokine (46). For example, with extreme exercise, IL-6 may be sufficiently produced by working muscle to increase circulating levels up to 100-fold (47) without signs of muscle tissue damage (48) or a change in IL-6 expressing immune cells (49). During exercise, IL-6 is released from muscle in response to low glycogen stores (50) or activation of AMPK, and acts through autocrine and paracrine mechanisms to increase fat oxidation, and enhance insulin-stimulated glucose uptake through GLUT4 translocation (51). As a myokine, IL-6 also provides an endocrine signal to enhance hepatic glucose production during exercise (52).

Importantly, IL-6 is produced as the predominant myokine in response to exercise and yet, as we observed it can also induce muscle dysfunction as part of the “cytokine storm” associated with IAV infection. We speculate that differences in the kinetics of IL-6 release and its association with other pro-inflammatory cytokines may underlie the differential response of muscle to IL-6. After exercise, IL-6 levels peak rapidly then fall (53, 54) while sustained elevations are present for days after influenza infection (27). Further, IL-6 generated during exercise is not accompanied by an increase in other cytokines elevated during influenza A infection (55). Our data are consistent with those of others who have shown that prolonged exposure to recombinant IL-6 can induce muscle atrophy (22, 56), and with observations from others that high levels of IL-6 are associated with the age-related decline in muscle function due to sarcopenia (57).

We found that pharmacologic inhibition of the IL-6 receptor using the FDA approved drug tocilizumab attenuated muscle loss during influenza A infection. We did not see adverse effects of tociluzumab in the muscle as there was no difference in muscle mass of the soleus and EDL. Furthermore, we saw no change in total body weight in mice treated with tocilizumab. Nevertheless, in health, IL-6 has an important role in maintenance of muscle bulk, modulating muscle carbohydrate and lipid metabolism (47, 58–60). The differing roles for IL-6 signaling in the muscle during health and disease are poorly understood, and suggest that the effects of IL-6 in the muscle might be modulated by other factors present in the muscle microenvironment during disease. Furthermore, influenza A-induced muscle loss was only partially inhibited by tocilizumab, suggesting that other cytokines released in response to influenza A infection (e.g. IL-1β, IL-18 and others), changes in inflammatory cell populations (e.g. Treg cells), or nutrient deprivation might independently contribute to muscle dysfunction (61–66). Influenza A infection in mice provides an excellent model system to further explore these possibilities.

We observed increased levels of atrogin-1 in muscle following influenza A infection, and heterozygous and homozygous loss of atrogin-1 resulted in a dose-dependent inhibition of influenza A induced muscle degradation. In cultured myotubes, the induction of atrogin-1 by IL-6 required the activation of STAT3 and FoxO3a, but not FoxO1. These data suggest inhibiting atrogin-1 directly or the pathways required for its induction may preserve muscle mass during influenza A infection. These results should be interpreted with some caution; however, as others have observed increased expression of mRNA for both *atrogin-1* and *MuRF1* in the skeletal muscle following influenza infection (67). Further, it is not clear whether the IL-6 and atrogin-1 mediated degradation of muscle proteins is adaptive process during influenza A infection. For example, the degradation of muscle proteins might provide metabolic substrates to fuel inflammatory cell responses to pathogen challenge. Alternatively, the systemic release of IL-6 might be a maladaptive consequence of the excessive inflammation thought to underlie the development of the multiple organ dysfunction syndrome. While our study does not answer this question, we saw no worsening in weight loss or mortality in influenza A infected atrogin-1 compared with wild type controls, nor did we observe any impact of tocilizumab on these parameters. However, tocilizumab has been associated transient neutropenia, increased body weight and elevated cholesterol in clinical trials (68, 69).

There are a number of limitations to this study. First, because the expression of atrogin-1 is largely limited to the muscle, the effects of atrogin-1 loss in other cells is less of a concern. However, it is possible that partial or complete developmental loss of atrogin-1 might activate pathways in *atrogin-1*$^{+/-}$ and *atrogin-1*$^{-/-}$ mice, respectively, which protect against influenza A-induced muscle loss. Further studies using inducible knockouts or pharmacologic inhibitors could address these concerns. Additionally, our model system is limited to infection with a single murine adapted influenza A virus. Studies using other strains of influenza A virus or administering tocilizumab to pigs, which are susceptible to circulating influenza A viruses could address this limitation. Finally, while IL-6 levels are often elevated in patients with ARDS secondary to other causes, the importance of IL-6 in muscle degradation in these conditions is unknown.

In summary, we provide evidence that influenza infection results in the release of IL-6 from the injured lung, which activates STAT3 and FoxO3a in the muscle to induce the expression of atrogin-1. Atrogin-1 is an E3 ligase that targets key muscle proteins for active degradation via the ubiquitin proteasome system. Thus, as depicted in Figure 6, IL-6 acts as an endocrine signal to promote active degradation of the skeletal muscle during influenza A pneumonia. Inhibition of the IL-6 receptor and genetic deletion of atrogin-1 attenuates the loss of muscle mass and function associated with influenza A infection, suggesting these pathways might be therapeutically targeted to preserve muscle mass in patients with influenza A-induced ARDS.

Acknowledgements

The authors wish to thank Angela Pantell and Marina Casalino Matsuda for their technical assistance. We are grateful to Regeneron Pharmaceuticals for providing the *atrogin-1* mice. Histology services were provided by the Northwestern University Mouse Histology and Phenotyping Laboratory, which is supported by NCI P30 CA060553 awarded to the Robert H Lurie Comprehensive Cancer Center. Imaging work was performed at the Northwestern University Center for Advanced Microscopy generously supported by NCI CCSG P30 CA060553 awarded to the Robert H Lurie Comprehensive Cancer Center.

This work was supported, in part, by grants from the National Institute on Aging PO1-AG-49665 and the National Institutes of Health HL-71643, T32-HL-076139.

Abbreviations used in this article:

IAV	influenza a virus
ARDS	acute respiratory distress syndrome
FoxO	forkhead box O
MuRF1	muscle RING finger 1
MAFbx/atrogin-1	muscle atrophy F-box protein
EDL	extensor digitorum longus
CSA	cross sectional area

References

1. 2010 Estimates of deaths associated with seasonal influenza --- United States, 1976–2007. MMWR Morb Mortal Wkly Rep 59: 1057–1062. [PubMed: 20798667]
2. Shrestha SS, Swerdlow DL, Borse RH, Prabhu VS, Finelli L, Atkins CY, Owusu-Edusei K, Bell B, Mead PS, Biggerstaff M, Brammer L, Davidson H, Jernigan D, Jhung MA, Kamimoto LA, Merlin TL, Nowell M, Redd SC, Reed C, Schuchat A, and Meltzer MI. 2011 Estimating the burden of 2009 pandemic influenza A (H1N1) in the United States (April 2009-April 2010). Clin Infect Dis 52 Suppl 1: S75–82. [PubMed: 21342903]
3. Kido H, Okumura Y, Takahashi E, Pan HY, Wang S, Yao D, Yao M, Chida J, and Yano M. 2012 Role of host cellular proteases in the pathogenesis of influenza and influenza-induced multiple organ failure. Biochim Biophys Acta 1824: 186–194. [PubMed: 21801859]
4. Jain S, Kamimoto L, Bramley AM, Schmitz AM, Benoit SR, Louie J, Sugerman DE, Druckenmiller JK, Ritger KA, Chugh R, Jasuja S, Deutscher M, Chen S, Walker JD, Duchin JS, Lett S, Soliva S, Wells EV, Swerdlow D, Uyeki TM, Fiore AE, Olsen SJ, Fry AM, Bridges CB, Finelli L, and A. V. H. I. T. Pandemic Influenza. 2009 Hospitalized patients with 2009 H1N1 influenza in the United States, April-June 2009. N Engl J Med 361: 1935–1944. [PubMed: 19815859]
5. Stevens RD, Dowdy DW, Michaels RK, Mendez-Tellez PA, Pronovost PJ, and Needham DM. 2007 Neuromuscular dysfunction acquired in critical illness: a systematic review. Intensive Care Med 33: 1876–1891. [PubMed: 17639340]
6. Walsh CJ, Batt J, Herridge MS, and Dos Santos CC. 2014 Muscle wasting and early mobilization in acute respiratory distress syndrome. Clin Chest Med 35: 811–826. [PubMed: 25453427]
7. Puthucheary ZA, Rawal J, McPhail M, Connolly B, Ratnayake G, Chan P, Hopkinson NS, Phadke R, Dew T, Sidhu PS, Velloso C, Seymour J, Agley CC, Selby A, Limb M, Edwards LM, Smith K, Rowlerson A, Rennie MJ, Moxham J, Harridge SD, Hart N, and Montgomery HE. 2013 Acute skeletal muscle wasting in critical illness. JAMA 310: 1591–1600. [PubMed: 24108501]
8. Herridge MS, Batt J, and Santos CD. 2014 ICU-acquired weakness, morbidity, and death. Am J Respir Crit Care Med 190: 360–362. [PubMed: 25127302]
9. Herridge MS, Tansey CM, Matte A, Tomlinson G, Diaz-Granados N, Cooper A, Guest CB, Mazer CD, Mehta S, Stewart TE, Kudlow P, Cook D, Slutsky AS, Cheung AM, and G. Canadian Critical Care Trials. 2011 Functional disability 5 years after acute respiratory distress syndrome. N Engl J Med 364: 1293–1304. [PubMed: 21470008]
10. Herridge MS, Cheung AM, Tansey CM, Matte-Martyn A, Diaz-Granados N, Al-Saidi F, Cooper AB, Guest CB, Mazer CD, Mehta S, Stewart TE, Barr A, Cook D, Slutsky AS, and G. Canadian Critical Care Trials. 2003 One-year outcomes in survivors of the acute respiratory distress syndrome. N Engl J Med 348: 683–693. [PubMed: 12594312]
11. Ceco E, Weinberg SE, Chandel NS, and Sznajder JI. 2017 Metabolism and Skeletal Muscle Homeostasis in Lung Disease. Am J Respir Cell Mol Biol 57: 28–34. [PubMed: 28085493]
12. Esteban A, Frutos-Vivar F, Muriel A, Ferguson ND, Peñuelas O, Abraira V, Raymondos K, Rios F, Nin N, Apezteguía C, Violi DA, Thille AW, Brochard L, González M, Villagomez AJ, Hurtado J, Davies AR, Du B, Maggiore SM, Pelosi P, Soto L, Tomicic V, D'Empaire G, Matamis D, Abroug F, Moreno RP, Soares MA, Arabi Y, Sandi F, Jibaja M, Amin P, Koh Y, Kuiper MA, Bülow H-H, Zeggwagh AA, and Anzueto A. 2013 Evolution of Mortality over Time in Patients Receiving Mechanical Ventilation. Am J Respir Crit Care Med 188: 220–230. [PubMed: 23631814]
13. Lilly CM, Cody S, Zhao H, Landry K, Baker SP, McIlwaine J, Chandler MW, Irwin RS, and G. University of Massachusetts Memorial Critical Care Operations. 2011 Hospital mortality, length of stay, and preventable complications among critically ill patients before and after tele-ICU reengineering of critical care processes. JAMA 305: 2175–2183. [PubMed: 21576622]
14. Kress JP, and Hall JB. 2014 ICU-acquired weakness and recovery from critical illness. N Engl J Med 370: 1626–1635. [PubMed: 24758618]
15. Lipshutz AK, and Gropper MA. 2013 Acquired neuromuscular weakness and early mobilization in the intensive care unit. Anesthesiology 118: 202–215. [PubMed: 22929731]

16. Tennila A, Salmi T, Pettila V, Roine RO, Varpula T, and Takkunen O. 2000 Early signs of critical illness polyneuropathy in ICU patients with systemic inflammatory response syndrome or sepsis. Intensive Care Med 26: 1360–1363. [PubMed: 11089765]

17. Dinglas VD, Aronson Friedman L, Colantuoni E, Mendez-Tellez PA, Shanholtz CB, Ciesla ND, Pronovost PJ, and Needham DM. 2017 Muscle Weakness and 5-Year Survival in Acute Respiratory Distress Syndrome Survivors. Crit Care Med 45: 446–453. [PubMed: 28067712]

18. Stitt TN, Drujan D, Clarke BA, Panaro F, Timofeyva Y, Kline WO, Gonzalez M, Yancopoulos GD, and Glass DJ. 2004 The IGF-1/PI3K/Akt pathway prevents expression of muscle atrophy-induced ubiquitin ligases by inhibiting FOXO transcription factors. Mol Cell 14: 395–403. [PubMed: 15125842]

19. Sandri M, Sandri C, Gilbert A, Skurk C, Calabria E, Picard A, Walsh K, Schiaffino S, Lecker SH, and Goldberg AL. 2004 Foxo transcription factors induce the atrophy-related ubiquitin ligase atrogin-1 and cause skeletal muscle atrophy. Cell 117: 399–412. [PubMed: 15109499]

20. Bodine SC, Latres E, Baumhueter S, Lai VK, Nunez L, Clarke BA, Poueymirou WT, Panaro FJ, Na E, Dharmarajan K, Pan ZQ, Valenzuela DM, DeChiara TM, Stitt TN, Yancopoulos GD, and Glass DJ. 2001 Identification of ubiquitin ligases required for skeletal muscle atrophy. Science 294: 1704–1708. [PubMed: 11679633]

21. Gomes MD, Lecker SH, Jagoe RT, Navon A, and Goldberg AL. 2001 Atrogin-1, a muscle-specific F-box protein highly expressed during muscle atrophy. Proc Natl Acad Sci U S A 98: 14440–14445. [PubMed: 11717410]

22. Baltgalvis KA, Berger FG, Pena MM, Davis JM, White JP, and Carson JA. 2009 Muscle wasting and interleukin-6-induced atrogin-I expression in the cachectic Apc (Min/+) mouse. Pflugers Arch 457: 989–1001. [PubMed: 18712412]

23. Bodell PW, Kodesh E, Haddad F, Zaldivar FP, Cooper DM, and Adams GR. 2009 Skeletal muscle growth in young rats is inhibited by chronic exposure to IL-6 but preserved by concurrent voluntary endurance exercise. J Appl Physiol (1985) 106: 443–453. [PubMed: 19057004]

24. Haddad F, Zaldivar F, Cooper DM, and Adams GR. 2005 IL-6-induced skeletal muscle atrophy. J Appl Physiol (1985) 98: 911–917. [PubMed: 15542570]

25. Knight D, Mutsaers SE, and Prele CM. 2011 STAT3 in tissue fibrosis: is there a role in the lung? Pulm Pharmacol Ther 24: 193–198. [PubMed: 20951825]

26. Oh HM, Yu CR, Dambuza I, Marrero B, and Egwuagu CE. 2012 STAT3 protein interacts with Class O Forkhead transcription factors in the cytoplasm and regulates nuclear/cytoplasmic localization of FoxO1 and FoxO3a proteins in CD4(+) T cells. J Biol Chem 287: 30436–30443. [PubMed: 22761423]

27. Hayden FG, Fritz R, Lobo MC, Alvord W, Strober W, and Straus SE. 1998 Local and systemic cytokine responses during experimental human influenza A virus infection. Relation to symptom formation and host defense. J Clin Invest 101: 643–649. [PubMed: 9449698]

28. Radigan KA, Urich D, Misharin AV, Chiarella SE, Soberanes S, Gonzalez A, Perlman H, Wunderink RG, Budinger GR, and Mutlu GM. 2012 The effect of rosuvastatin in a murine model of influenza A infection. PLoS One 7: e35788. [PubMed: 22536437]

29. Parsons PE, Eisner MD, Thompson BT, Matthay MA, Ancukiewicz M, Bernard GR, Wheeler AP, and N. A. R. D. S. C. T. Network. 2005 Lower tidal volume ventilation and plasma cytokine markers of inflammation in patients with acute lung injury. Crit Care Med 33: 1–6; discussion 230–232. [PubMed: 15644641]

30. Agrawal A, Zhuo H, Brady S, Levitt J, Steingrub J, Siegel MD, Soto G, Peterson MW, Chesnutt MS, Matthay MA, and Liu KD. 2012 Pathogenetic and predictive value of biomarkers in patients with ALI and lower severity of illness: results from two clinical trials. Am J Physiol Lung Cell Mol Physiol 303: L634–639. [PubMed: 22865551]

31. Short KR, Kroeze EJ, Fouchier RA, and Kuiken T. 2014 Pathogenesis of influenza-induced acute respiratory distress syndrome. Lancet Infect Dis 14: 57–69. [PubMed: 24239327]

32. Chiarella SE, Soberanes S, Urich D, Morales-Nebreda L, Nigdelioglu R, Green D, Young JB, Gonzalez A, Rosario C, Misharin AV, Ghio AJ, Wunderink RG, Donnelly HK, Radigan KA, Perlman H, Chandel NS, Budinger GR, and Mutlu GM. 2014 beta2-Adrenergic agonists augment

air pollution-induced IL-6 release and thrombosis. J Clin Invest 124: 2935–2946. [PubMed: 24865431]

33. Mutlu GM, Green D, Bellmeyer A, Baker CM, Burgess Z, Rajamannan N, Christman JW, Foiles N, Kamp DW, Ghio AJ, Chandel NS, Dean DA, Sznajder JI, and Budinger GR. 2007 Ambient particulate matter accelerates coagulation via an IL-6-dependent pathway. J Clin Invest 117: 2952–2961. [PubMed: 17885684]
34. Jaitovich A, Angulo M, Lecuona E, Dada LA, Welch LC, Cheng Y, Gusarova G, Ceco E, Liu C, Shigemura M, Barreiro E, Patterson C, Nader GA, and Sznajder JI. 2015 High CO2 levels cause skeletal muscle atrophy via AMP-activated kinase (AMPK), FoxO3a protein, and muscle-specific Ring finger protein 1 (MuRF1). J Biol Chem 290: 9183–9194. [PubMed: 25691571]
35. Meyer OA, Tilson HA, Byrd WC, and Riley MT. 1979 A method for the routine assessment of fore- and hindlimb grip strength of rats and mice. Neurobehav Toxicol 1: 233–236. [PubMed: 551317]
36. Schindelin J, Arganda-Carreras I, Frise E, Kaynig V, Longair M, Pietzsch T, Preibisch S, Rueden C, Saalfeld S, Schmid B, Tinevez JY, White DJ, Hartenstein V, Eliceiri K, Tomancak P, and Cardona A. 2012 Fiji: an open-source platform for biological-image analysis. Nat Methods 9: 676–682. [PubMed: 22743772]
37. Radigan KA, Morales-Nebreda L, Soberanes S, Nicholson T, Nigdelioglu R, Cho T, Chi M, Hamanaka RB, Misharin AV, Perlman H, Budinger GR, and Mutlu GM. 2014 Impaired clearance of influenza A virus in obese, leptin receptor deficient mice is independent of leptin signaling in the lung epithelium and macrophages. PLoS One 9: e108138. [PubMed: 25232724]
38. Andres-Mateos E, Mejias R, Soleimani A, Lin BM, Burks TN, Marx R, Lin B, Zellars RC, Zhang Y, Huso DL, Marr TG, Leinwand LA, Merriman DK, and Cohn RD. 2012 Impaired skeletal muscle regeneration in the absence of fibrosis during hibernation in 13-lined ground squirrels. PLoS One 7: e48884. [PubMed: 23155423]
39. Bradford MM 1976 A rapid and sensitive method for the quantitation of microgram quantities of protein utilizing the principle of protein-dye binding. Anal Biochem 72: 248–254. [PubMed: 942051]
40. Dada LA, Trejo Bittar HE, Welch LC, Vagin O, Deiss-Yehiely N, Kelly AM, Baker MR, Capri J, Cohn W, Whitelegge JP, Vadasz I, Gruenbaum Y, and Sznajder JI. 2015 High CO2 Leads to Na,K-ATPase Endocytosis via c-Jun Amino-Terminal Kinase-Induced LMO7b Phosphorylation. Mol Cell Biol 35: 3962–3973. [PubMed: 26370512]
41. Schneider CA, Rasband WS, and Eliceiri KW. 2012 NIH Image to ImageJ: 25 years of image analysis. Nat Methods 9: 671–675. [PubMed: 22930834]
42. Nishimoto N, and Kishimoto T. 2008 Humanized antihuman IL-6 receptor antibody, tocilizumab. Handb Exp Pharmacol: 151–160. [PubMed: 18071945]
43. Lee JJ, Waak K, Grosse-Sundrup M, Xue F, Lee J, Chipman D, Ryan C, Bittner EA, Schmidt U, and Eikermann M. 2012 Global muscle strength but not grip strength predicts mortality and length of stay in a general population in a surgical intensive care unit. Phys Ther 92: 1546–1555. [PubMed: 22976446]
44. Hermans G, Van Mechelen H, Clerckx B, Vanhullebusch T, Mesotten D, Wilmer A, Casaer MP, Meersseman P, Debaveye Y, Van Cromphaut S, Wouters PJ, Gosselink R, and Van den Berghe G. 2014 Acute outcomes and 1-year mortality of intensive care unit-acquired weakness. A cohort study and propensity-matched analysis. Am J Respir Crit Care Med 190: 410–420. [PubMed: 24825371]
45. dos Santos C, Hussain SNA, Mathur S, Picard M, Herridge M, Correa J, Bain A, Guo Y, Advani A, Advani SL, Tomlinson G, Katzberg H, Streutker CJ, Cameron JI, Schols A, Gosker H, and Batt J. 2016 Mechanisms of Chronic Muscle Wasting and Dysfunction After an Intensive Care Unit Stay: A Pilot Study. Am J Respir Crit Care Med 194: 821–830. [PubMed: 27058306]
46. Pedersen BK, Bruunsgaard H, Ostrowski K, Krabbe K, Hansen H, Krzywkowski K, Toft A, Sondergaard SR, Petersen EW, Ibfelt T, and Schjerling P. 2000 Cytokines in aging and exercise. Int J Sports Med 21 Suppl 1: S4–9. [PubMed: 10893017]
47. Steensberg A, Keller C, Starkie RL, Osada T, Febbraio MA, and Pedersen BK. 2002 IL-6 and TNF-alpha expression in, and release from, contracting human skeletal muscle. Am J Physiol Endocrinol Metab 283: E1272–1278. [PubMed: 12388119]

48. Fischer CP 2006 Interleukin-6 in acute exercise and training: what is the biological relevance? Exerc Immunol Rev 12: 6–33. [PubMed: 17201070]
49. Starkie RL, Rolland J, Angus DJ, Anderson MJ, and Febbraio MA. 2001 Circulating monocytes are not the source of elevations in plasma IL-6 and TNF-alpha levels after prolonged running. Am J Physiol Cell Physiol 280: C769–774. [PubMed: 11245592]
50. Ruderman NB, Keller C, Richard AM, Saha AK, Luo Z, Xiang X, Giralt M, Ritov VB, Menshikova EV, Kelley DE, Hidalgo J, Pedersen BK, and Kelly M. 2006 Interleukin-6 regulation of AMP-activated protein kinase. Potential role in the systemic response to exercise and prevention of the metabolic syndrome. Diabetes 55 Suppl 2: S48–54. [PubMed: 17130644]
51. Carey AL, Steinberg GR, Macaulay SL, Thomas WG, Holmes AG, Ramm G, Prelovsek O, Hohnen-Behrens C, Watt MJ, James DE, Kemp BE, Pedersen BK, and Febbraio MA. 2006 Interleukin-6 increases insulin-stimulated glucose disposal in humans and glucose uptake and fatty acid oxidation in vitro via AMP-activated protein kinase. Diabetes 55: 2688–2697. [PubMed: 17003332]
52. Febbraio MA, Hiscock N, Sacchetti M, Fischer CP, and Pedersen BK. 2004 Interleukin-6 is a novel factor mediating glucose homeostasis during skeletal muscle contraction. Diabetes 53: 1643–1648. [PubMed: 15220185]
53. Fischer CP, Plomgaard P, Hansen AK, Pilegaard H, Saltin B, and Pedersen BK. 2004 Endurance training reduces the contraction-induced interleukin-6 mRNA expression in human skeletal muscle. Am J Physiol Endocrinol Metab 287: E1189–1194. [PubMed: 15304377]
54. Ostrowski K, Hermann C, Bangash A, Schjerling P, Nielsen JN, and Pedersen BK. 1998 A trauma-like elevation of plasma cytokines in humans in response to treadmill running. J Physiol 513 (Pt 3): 889–894. [PubMed: 9824725]
55. Pedersen BK, and Febbraio MA. 2008 Muscle as an endocrine organ: focus on muscle-derived interleukin-6. Physiol Rev 88: 1379–1406. [PubMed: 18923185]
56. Goodman MN 1994 Interleukin-6 induces skeletal muscle protein breakdown in rats. Proc Soc Exp Biol Med 205: 182–185. [PubMed: 8108469]
57. Schaap LA, Pluijm SM, Deeg DJ, and Visser M. 2006 Inflammatory markers and loss of muscle mass (sarcopenia) and strength. Am J Med 119: 526 e529–517.
58. Febbraio MA, and Pedersen BK. 2002 Muscle-derived interleukin-6: mechanisms for activation and possible biological roles. FASEB J 16: 1335–1347. [PubMed: 12205025]
59. Steensberg A, Febbraio MA, Osada T, Schjerling P, van Hall G, Saltin B, and Pedersen BK. 2001 Interleukin-6 production in contracting human skeletal muscle is influenced by pre-exercise muscle glycogen content. J Physiol 537: 633–639. [PubMed: 11731593]
60. Pedersen M, Bruunsgaard H, Weis N, Hendel HW, Andreassen BU, Eldrup E, Dela F, and Pedersen BK. 2003 Circulating levels of TNF-alpha and IL-6-relation to truncal fat mass and muscle mass in healthy elderly individuals and in patients with type-2 diabetes. Mech Ageing Dev 124: 495–502. [PubMed: 12714258]
61. Kuswanto W, Burzyn D, Panduro M, Wang KK, Jang YC, Wagers AJ, Benoist C, and Mathis D. 2016 Poor Repair of Skeletal Muscle in Aging Mice Reflects a Defect in Local, Interleukin-33-Dependent Accumulation of Regulatory T Cells. Immunity 44: 355–367. [PubMed: 26872699]
62. Zhang Y, Sun H, Fan L, Ma Y, Sun Y, Pu J, Yang J, Qiao J, Ma G, and Liu J. 2012 Acute respiratory distress syndrome induced by a swine 2009 H1N1 variant in mice. PLoS One 7: e29347. [PubMed: 22235288]
63. Thomas PG, Dash P, Aldridge JR, Jr., Ellebedy AH, Reynolds C, Funk AJ, Martin WJ, Lamkanfi M, Webby RJ, Boyd KL, Doherty PC, and Kanneganti TD. 2009 The intracellular sensor NLRP3 mediates key innate and healing responses to influenza A virus via the regulation of caspase-1. Immunity 30: 566–575. [PubMed: 19362023]
64. Allen IC, Scull MA, Moore CB, Holl EK, McElvania-TeKippe E, Taxman DJ, Guthrie EH, Pickles RJ, and Ting JP. 2009 The NLRP3 inflammasome mediates in vivo innate immunity to influenza A virus through recognition of viral RNA. Immunity 30: 556–565. [PubMed: 19362020]
65. Ichinohe T, Pang IK, and Iwasaki A. 2010 Influenza virus activates inflammasomes via its intracellular M2 ion channel. Nat Immunol 11: 404–410. [PubMed: 20383149]

66. Wang S, Le TQ, Kurihara N, Chida J, Cisse Y, Yano M, and Kido H. 2010 Influenza virus-cytokine-protease cycle in the pathogenesis of vascular hyperpermeability in severe influenza. J Infect Dis 202: 991–1001. [PubMed: 20731583]

67. Bartley JM, Pan SJ, Keilich SR, Hopkins JW, Al-Naggar IM, Kuchel GA, and Haynes L. 2016 Aging augments the impact of influenza respiratory tract infection on mobility impairments, muscle-localized inflammation, and muscle atrophy. Aging (Albany NY) 8: 620–635. [PubMed: 26856410]

68. Wright HL, Cross AL, Edwards SW, and Moots RJ. 2014 Effects of IL-6 and IL-6 blockade on neutrophil function in vitro and in vivo. Rheumatology (Oxford) 53: 1321–1331. [PubMed: 24609058]

69. Genovese MC, McKay JD, Nasonov EL, Mysler EF, da Silva NA, Alecock E, Woodworth T, and Gomez-Reino JJ. 2008 Interleukin-6 receptor inhibition with tocilizumab reduces disease activity in rheumatoid arthritis with inadequate response to disease-modifying antirheumatic drugs: the tocilizumab in combination with traditional disease-modifying antirheumatic drug therapy study. Arthritis Rheum 58: 2968–2980. [PubMed: 18821691]

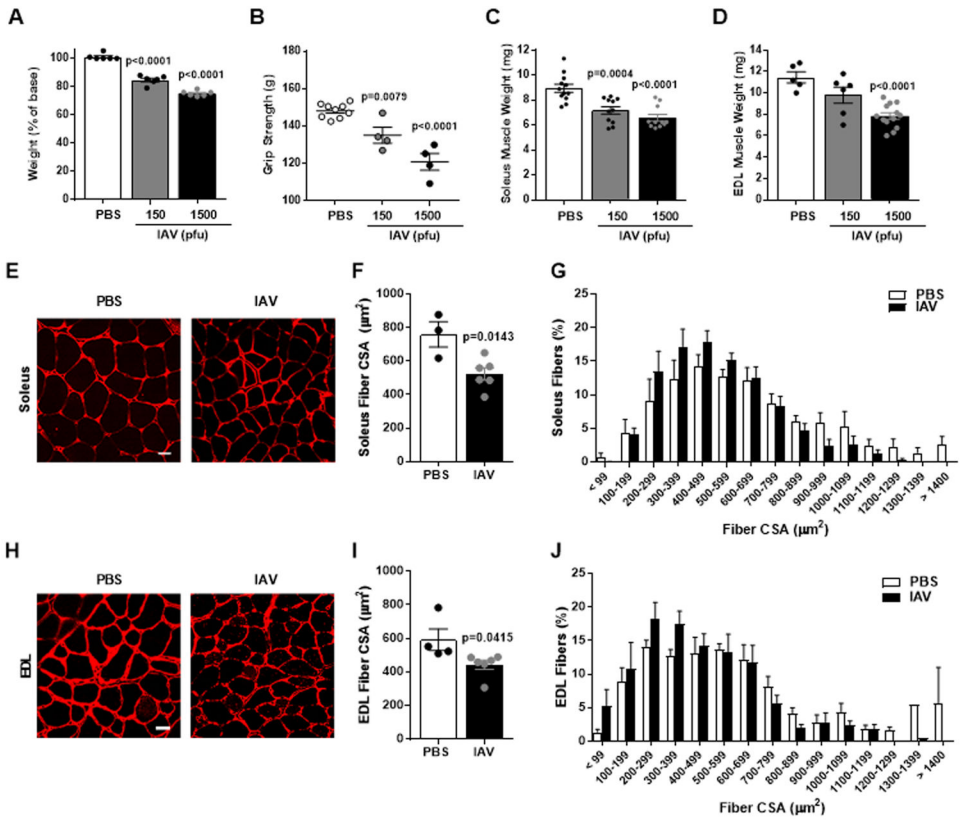

Figure 1. Wild-type mice lose muscle weight and strength after influenza infection and have reduced cross-sectional area (CSA) after influenza infection.

Adult male C57Bl/6 mice were infected with 150 or 1500 pfu/mouse of influenza A Virus (IAV) or PBS (control) and 7 days post-infection **(A)** total body weight (n=6 mice/group) and **(B)** fore-limb grip strength were determined (n= 4-9 mice/group). **(C)** Soleus (n= 11-12 mice/group) and **(D)** EDL (n= 5-13 mice/group) wet muscle weights were determined after muscles were excised, frozen and cryosectioned. **(E-J)**Soleus and EDL CSA were determined using cross-sections immunostained for laminin. **(E, H)**Representative images are shown. (40X magnification) Scale Bars = 20 μm. **(F)** Mean soleus fiber CSA (n=3-6 mice/group) and**(G)** a histogram depicting the fiber size distribution. **(I)**Mean EDL fiber CSA (n=4-6 mice/group) and**(J)** histogram depicting the fiber size distribution. Bars represent means ± SEM. n ≥ 3 of at least 3 independent experiments. A one-way ANOVA with Dunnett's post-hoc corrections for comparison with more than 3 groups and a Student's *t*-test between two groups were used to show statistical differences. All groups are compared to the control PBS-treated and p-values are shown.

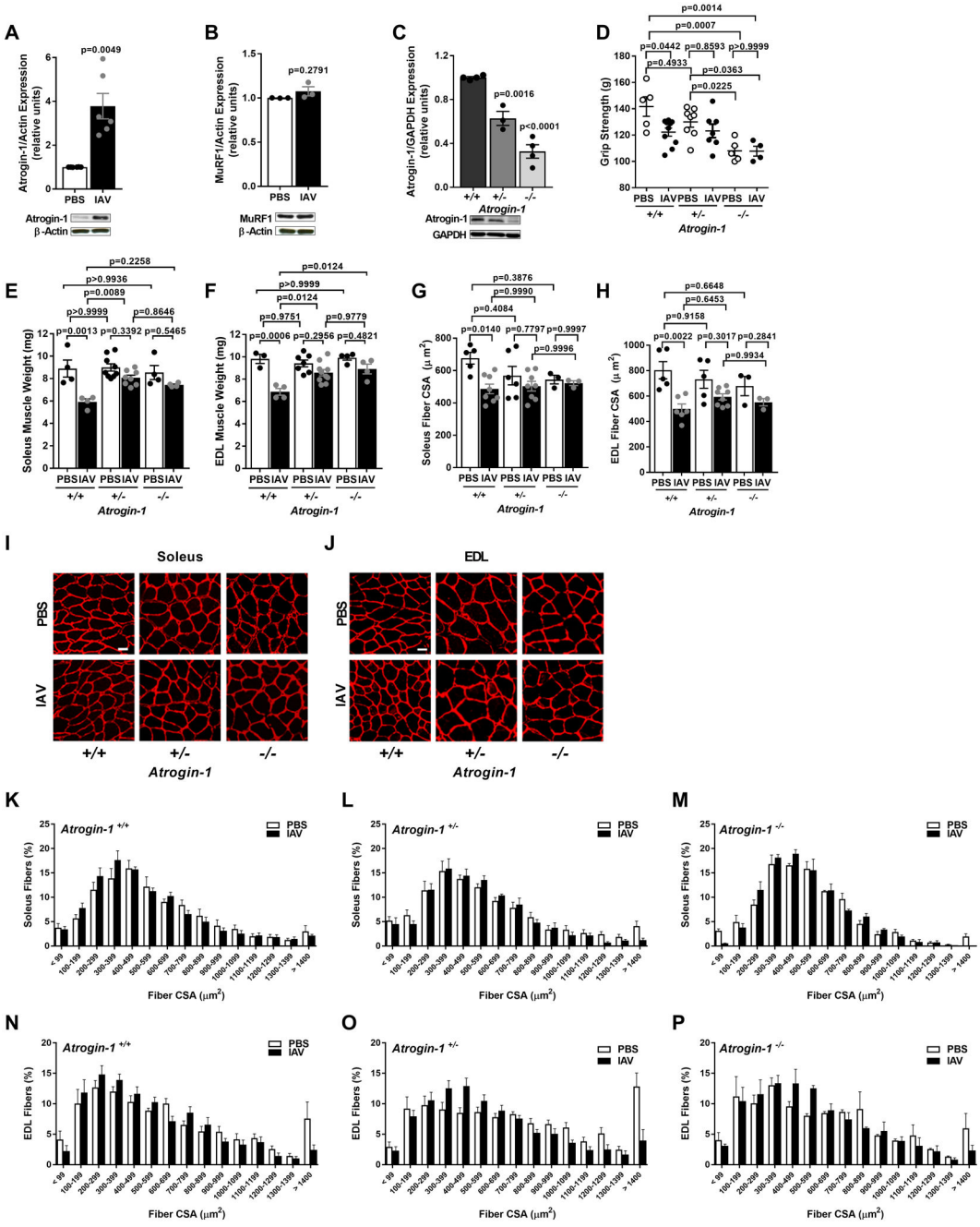

Figure 2. Influenza-induced muscle dysfunction is attenuated in mice with genetic loss of atrogin-1.

(A-B) Adult male C57Bl/6 mice were infected with 1500 pfu/mouse of influenza A Virus (IAV) or PBS (control) and 7 days post-infection soleus muscles were excised and atrogin-1 (n=6 mice/group) and MuRF1 (n=3 mice/group) expression was determined by Western blot. β-actin was used as loading control. A Student's *t*-test between two groups was used to show statistical differences. **(C)** Soleus muscle from *atrogin-1* ($^{+/+}$, $^{+/-}$ and $^{-/-}$) mice were excised and atrogin-1 expression was determined by Western blot. GAPDH was used as loading control. (n=3-4 mice/group). A one-way ANOVA with Dunnett's post-hoc

corrections for comparison with more than 3 groups was used to show statistical differences. **(D-P)** *Atrogin-1*($^{+/+, +/-}$ and $^{-/-}$) mice infected with 1500 pfu/mouse of influenza A Virus (IAV) or PBS (control) and 7 days post-infection **(D)** fore-limb grip strength was determined. (n=4-10 animals/group). A one-way ANOVA with Tukey's post-hoc corrections for comparison with more than 3 groups was used to show statistical differences. **(E)** Soleus (n=4-9 animals/group) and **(F)** EDL (n=3-9 groups/group) wet muscle weight were determined after muscles were excised, frozen and cryosectioned. A one-way ANOVA with Tukey's post-hoc corrections for comparison with more than 3 groups was used to show statistical differences. **(G-P)** Soleus (n=3-8 mice/group) and EDL (n=3–8 mice/group) cross sectional area (CSA) were determined using muscle cross-sections immunostained for laminin. A one-way ANOVA with Tukey's post-hoc corrections for comparison with more than 3 groups was used to show statistical differences. **(G-H)** Meansoleus and EDL fiber CSA are shown. **(I-J)** Representative images are shown. (40X magnification) Scale Bars = 20 μm. **(K-P)** Histograms depicting the fiber size distribution for soleus muscle of **(K)** *Atrogin-1*$^{+/+}$ **(L)** *Atrogin-1*$^{+/-}$ *and* **(M)** *Atrogin-1*$^{-/-}$and EDL muscles of **(N)** *Atrogin-1*$^{+/+}$ **(O)** *Atrogin-1*$^{+/-}$ *and* **(P)** *Atrogin-1*$^{-/-}$. Bars represent means ± SEM and p-values are shown. n ≥ 3 from at least 3 independent experiments.

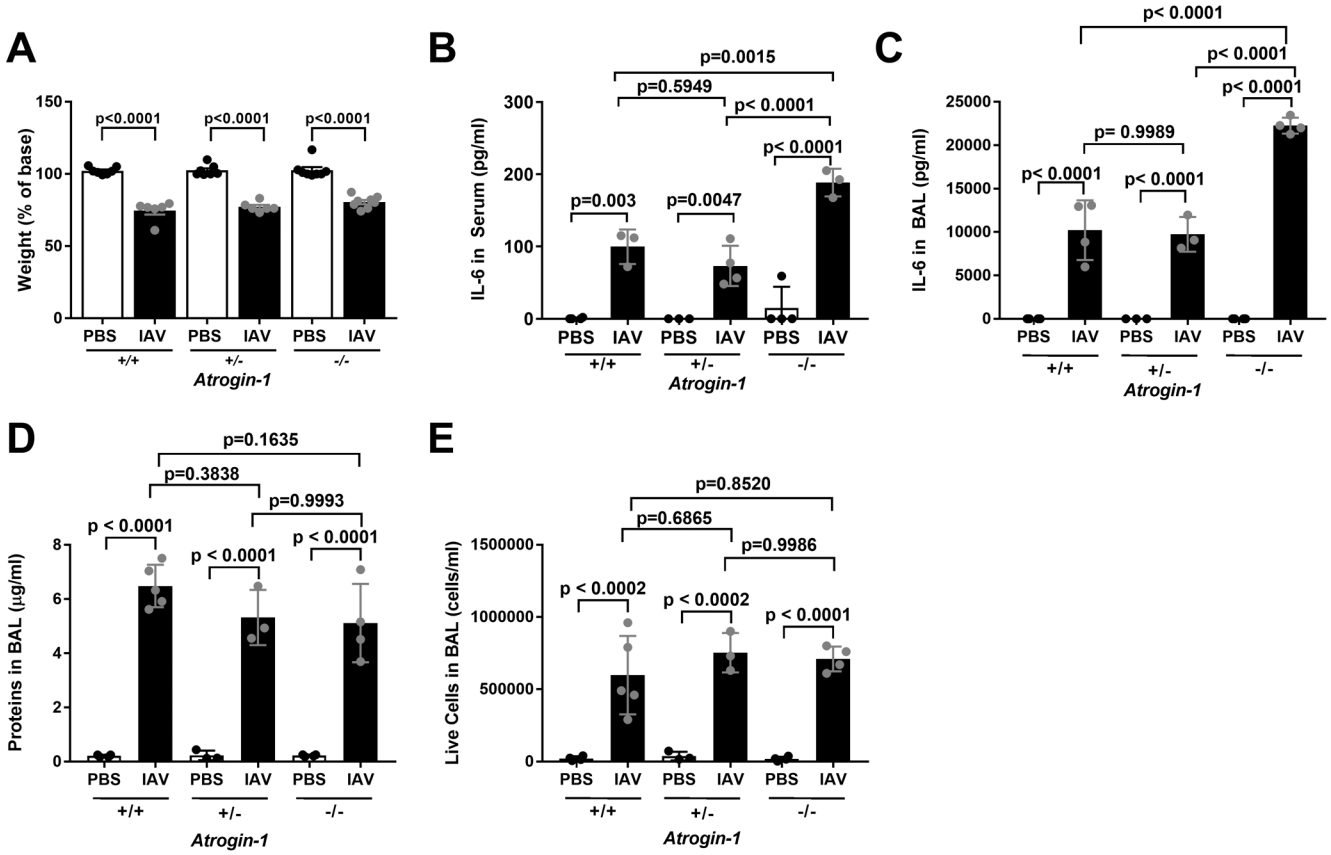

Figure 3. Influenza-induced body weight is attenuated and IL-6 is increased in serum and broncholalveolar lavage fluid in mice with genetic loss of atrogin-1.

Adult male *atrogin-1* ($^{+/+, +/-}$ and $^{-/-}$) mice were infected with 1500 pfu/mouse of influenza A Virus (IAV) or PBS (control) and 7 days post-infection total body weight was assessed (n=6-8 mice/group). **(B)** IL-6 was measured by ELISA in the serum. **(C)** IL-6 was measured by ELISA in the bronchoalveolar lavage (BAL) fluid. **(D)** Live cells in BAL fluid were measured by trypan blue exclusion. **(E)** Proteins in BAL fluid were measured by Bradford Assay. (n=3-5 mice/group). Bars represent means ± SEM and p-values are shown. A one-way ANOVA with Tukey's post-hoc corrections for comparison with more than 3 groups was used to show statistical differences. n ≥ 3 from at least 3 independent experiments.

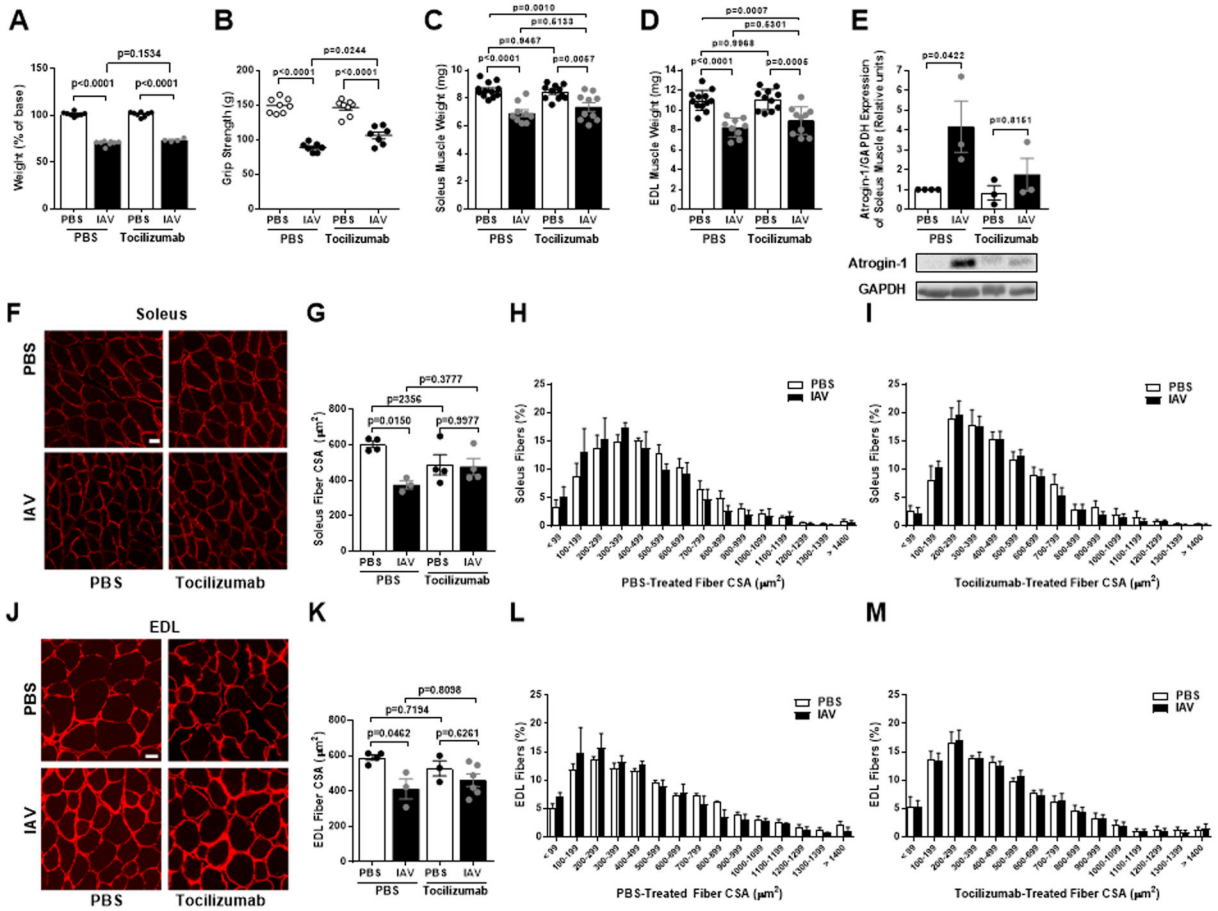

Figure 4. The IL-6-receptor antibody tocilizumab attenuates influenza-induced muscle dysfunction.

Adult male wildtype C57Bl/6 mice were pre-treated with the interleukin-6 (IL-6) receptor antibody, tocilizumab (8 mg/kg), 24 hours later infected with 1500 pfu/mouse of influenza A Virus (IAV) or PBS (control) and 7 days post-infection **(A)** total body weight (n=4-8 mice/group). **(B)** fore-limb grip strength was determined (n=7-8 mice/group). **(C)** Soleus (n=9-12 mice/group) and **(D)** EDL (n=10-12 mice/group) wet muscle weight were determined after muscles were excised, frozen and cryosectioned. For A-D, a one-way ANOVA with Tukey's post-hoc corrections for comparison with more than 3 groups was used to show statistical differences. The p-values are shown. **(E)** Quantification and representative Western blot of atrogin-1 expression in the mouse soleus muscle of PBS and tocilizumab-treated mice (n=3 mice/group). A one-way ANOVA with Dunnett's post-hoc corrections for comparison with more than 3 groups was used to show statistical differences. All groups are compared to the control PBS-treated and p-value is shown. **(F-M)** Muscle cross-sections immunostained for laminin antibody were used to determine the mean soleus and EDL fiber cross-sectional area (CSA). **(F, J)**Representative images are shown. (40X magnification) Scale Bars = 20 μm. **(G)** Soleus (n=4 mice/group) and **(K)** EDL (n=3-6 mice/group) mean fiber cross-sectional area (CSA) are shown. A one-way ANOVA with Tukey's post-hoc corrections for comparison with more than 3 groups was used to show statistical differences. **(H-I, L-M)** Histograms depicting the fiber size distribution are shown for **(H-I)** soleus and **(L-M)** EDL

mice treated with PBS or tocilizumab prior to influenza infection. Bars represent means ± SEM and p-values are shown. n ≥ 3 of at least 3 independent experiments.

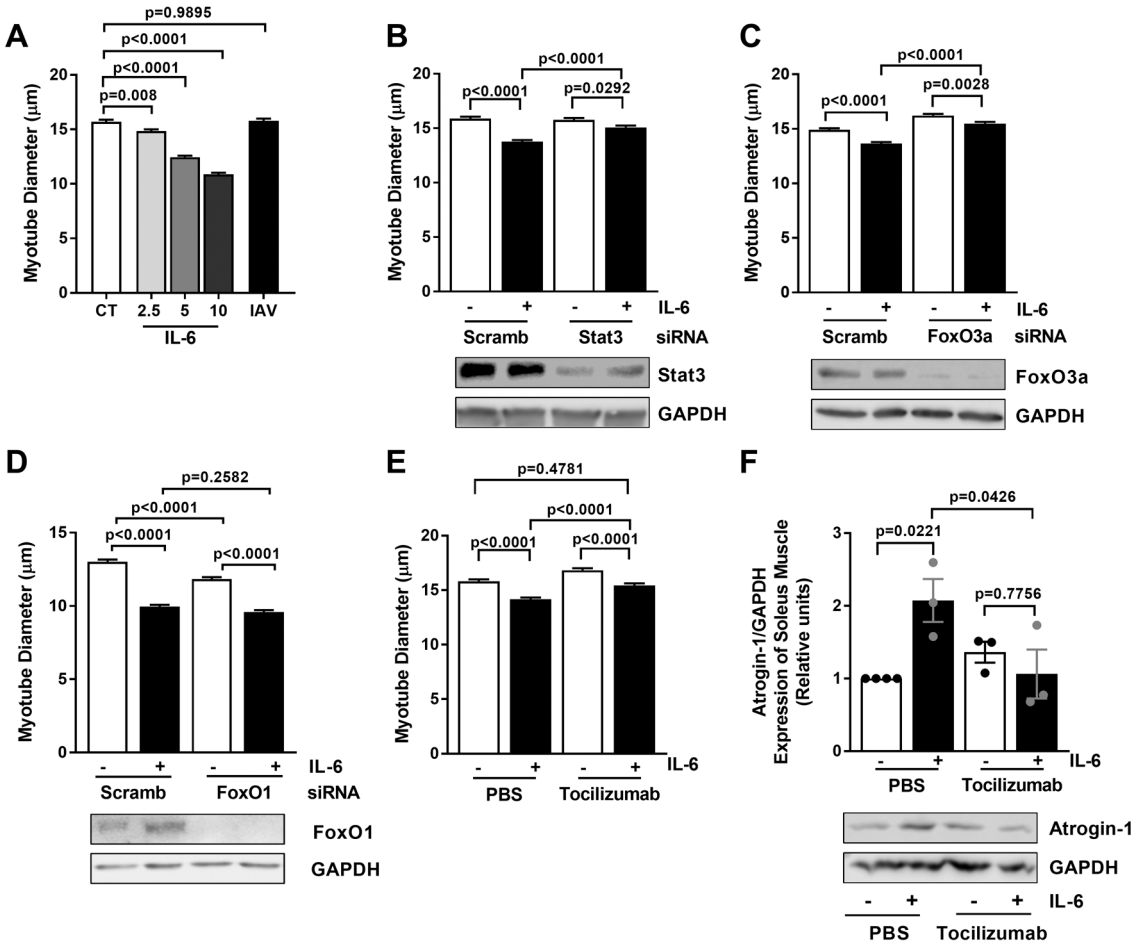

Figure 5. IL-6 acts via STAT3, FoxO3a, and Atrogin1 to induce skeletal muscle dysfunction.

(A) C2C12 myotubes were treated with recombinant IL-6 (2.5, 5, 10 ng/ml) or infected with 2 MOI IAV on Day 4 of differentiation for 16 hours. Phase contrast images were acquired on Day 5 of differentiation. Graph depicts average myotube diameters (~375 measurements/group; from at least 4 independent experiments). A one-way ANOVA with Dunnett's post-hoc corrections for comparison with more than 3 groups was used to show statistical differences. All groups are compared to the control (CT) and p-value is shown. **(B-D)** Myotubes were transfected with scrambled (Scramb), *STAT3* (~425 measurements/group; from at least 3 independent experiments), *FoxO3a*(~ 625 measurements/group; from at least 5 independent experiments) or *FoxO1* (~ 679 measurements/group; from at least 4 independent experiments) siRNA on Day 2 of differentiation followed by recombinant IL-6 treatment (10 ng/ml) on Day 4. Phase contrast images were obtained and cell lysates were analyzed on Day 5 of differentiation. Upper panel shows graph depicting average myotube diameter while lower panel depicts Western blot showing knock-down efficiency. GAPDH is shown as loading control. A one-way ANOVA with Tukey's post-hoc corrections for comparison with more than 3 groups was used to show statistical differences. (**D-E)** C2C12 myotubes were treated with tocilizumab 10 μg/ml on Day 3 of differentiation for 24 hours followed by treatment with recombinant mouse IL-6 for 16 hours. **(E)** Graph depicts average myotube diameter (~475 measurements/group; from at least 4 independent experiments). A

one-way ANOVA with Tukey's post-hoc corrections for comparison with more than 3 groups was used to show statistical differences. **(F)** Quantification and representative Western blot of atrogin-1 expression in C2C12 myotubes. GAPDH is shown as loading control (n=3 mice/group). Bars represent means ± SEM and p-values are shown.

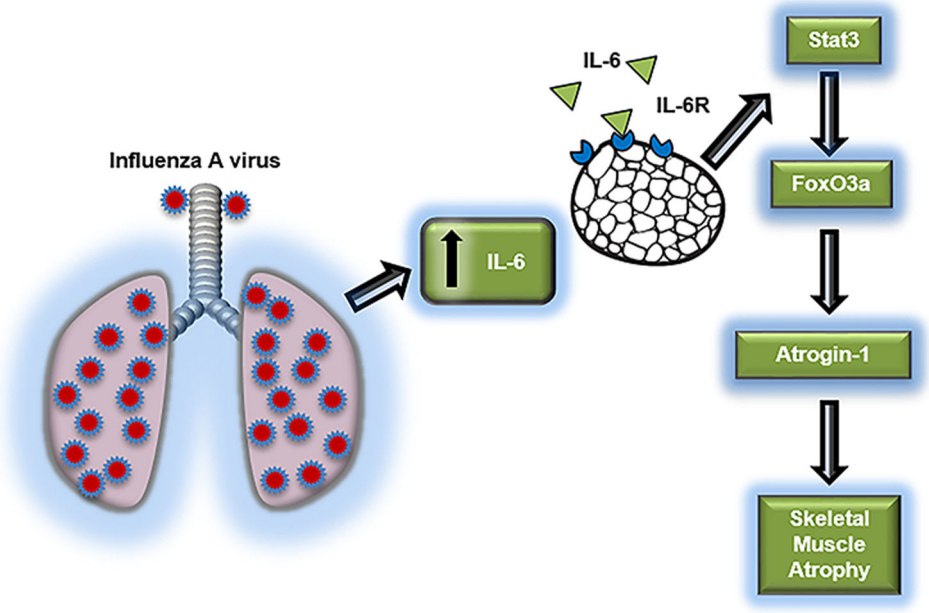

Figure 6.

In a murine model of influenza A infection, the release of IL-6 leads to the up regulation of the E3 ligase atrogin-1 leading to skeletal muscle dysfunction.